Journal of Soft Computing and Information Technology (JSCIT)
Babol Noshirvani University of Technology, Babol, Iran
Journal Homepage: www.jscit.nit.ac.ir
DOI:
Volume *, Number *, Season 20**, pp. 1-7
Received: 2016/02/06; Revised: 2017/06/13; Accepted: 2017/09/06

Image Denoising Based on a Local Optimal Balance between Fidelity and Smoothness

Arefeh Khanlari and Mehdi Ezoji
Department of Electronics, Faculty of Electrical and Computer Engineering
Babol Noshirvani university of technology, Babol, Mazandaran, Iran
a.khanlari@stu.nit.ac.ir, m.ezoji@nit.ac.ir

Corresponding author address: Mehdi Ezoji, Faculty of Electrical and Computer Engineering, Babol Noshirvani University of Technology, Babol, Iran, Post Code : 47148 – 71167.

Abstract- This paper addresses image denoising problem based on minimization of an appropriate energy function. This energy function consists of data fidelity term and targeted smoothness term. In this paper, a local optimal balance between these two terms is considered. This strategy leads to image invariant denoising and also preserve edges simultanously. Experimental results verify the effectiveness of this approach.

Keywords- Image Denoising, Energy Function, Local Balance, Fidelity and Smoothness.

.

I. INTRODUCTION

Image denoising is an important research area and an actual foundation for many applications, such as object recognition, digital entertainment, and remote sensing imaging. Denoising techniques have become a critical step for improving the final visual quality of images.

Denoising is the process of reconstructing the original image by removing unwanted noise from an observed image. It is designed to suppress the noise, while preserving the image structures and details as much as possible. The main challenge is to design noise reduction filters that provide a compromise between these two purposes.

In most cases, we have such an image formation model as follows [1-4]:

$$y(x) = z(x) + v(x) \quad (1)$$

where x is the 2D spatial coordinates of pixels in an image. z and y are the true and observed images repectively. v is the independent additive white noise, which is assumed to be a zero mean normally distributed variable with a standard deviation σ.

Generally, image denoising approaches can be categorized as spatial domain, transform domain, and dictionary learning based as shown in Fig. 1.

Spatial domain filters exploit spatial correlations in images. The spatial filters are classified into two categories i.e. local and nonlocal filters.

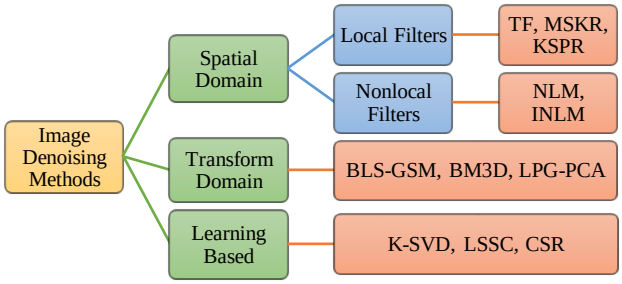

Fig. 1: Taxonomy of state-of-the-art denoising methods [1].

In local filtering, the candidate patch selection process is restricted by the spatial distance (e.g. trained filter (TF) [2]). A filter is nonlocal if the candidate patch selection depends only on the similarity and is not restricted by the spatial distance (e.g. Nonlocal means (NLM) [3]). There are some variational formulation of the non-local similarity in [4-5]. [6-9] addressed the image denoising problem using connecting the graph-based signal representation and

associated Laplacian matrix with non-local similarity. [10] proposed a nonlinear fractional differential filter mask for image denoising. In [11] a low-order variational model based on the splitting technique for regularize was proposed.

The second category is transform domain methods in which the image patches are represented by the orthonormal basis (e.g. wavelets [11]) with a series of coefficients. The smaller coefficients are related to the high frequency part of the input image corresponding to image details and noise. After adjusting these smaller coefficients, the reconstructed image could have less noise.

The general idea of dictionary learning based methods (e.g. the K-clustering with singular value decomposition (K-SVD) [13]) is that they perform denoising by learning a large group/dictionary of patches from an image dataset. Then each patch in the estimated image can be expressed as a linear combination of only few patches from this redundant dictionary. To improve the accuracy of the sparse representation-based algorithms, adaptive patch search (APS) and using various image priors are proposed in [14-16]. Weighted joint sparse representation, [17] is proposed to removing the mixed noise in images.

The proposed algorithm in this paper falls into the first category and is considered as a nonlocal filter.

The remainder of this paper is organized as follows: In section II, the basic algorithms and the proposed approach are described. In section III, the experiments and evaluations are discussed. Finally, the conclusion is drawn in section IV.

II. PROPOSED ALGORITHM

The idea of the proposed algorithm in this paper is based on the facts provided in [9, 18]. Therefore we start with a brief description of these image denoising algorithms as prerequisites information.

A. Basic Algorithms

- Image denoising problem in [18] leads to minimizing the following energy function:

$$E(z) = \sum_{i=1}^{n} |z_i - y_i|^2 + \sum_{i=1}^{n} \sum_{j \in N(i)} k_{ij} |z_i - z_j|^2 \qquad (2)$$

Which the first term on the right-hand side is called the data fidelity term and the second one is the smoothness term.

Minimization of (2) leads to the following closed form solution:

$$\boldsymbol{z} = [I + 2(D - K)]^{-1} \boldsymbol{y} \qquad (3)$$

where the (i, j)th element of matrix K demonstrates the degree of similarity between pixels i and j which is computed from Eq. (4). D is a diagonal matrix whose ith diagonal element is the sum of the elements of ith row of K.

$$k_{ij} = \begin{cases} a.\exp\left(-\frac{\Delta(i,j)}{b}\right).\Gamma(i,j).T(i,j) & i \neq j,\ j \in N(i) \\ 0 & i \neq j,\ j \notin N(i) \\ c & i = j \end{cases} \qquad (4)$$

where Δ(i,j) and Γ(i,j) are defined as:

$$\Delta(i,j) = |y_i - y_j|^2 \qquad (5)$$

$$\Gamma(i,j) = \exp\left(-\frac{|i-j|^2}{2}\right) \qquad (6)$$

To preserving the edges, similarity matrix K carries region adjacency information. According to the output of Canny edge detector, if pixels i and j have the same region indexes ($C_i = C_j$) then $T(C_i = C_j) = 1$ and 0 otherwise.

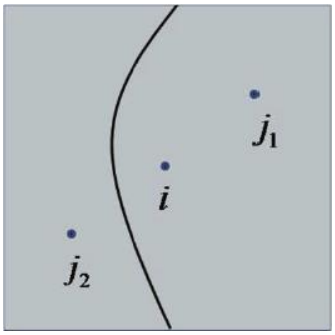

Fig 1: Explanation of the region indexes. The curve denotes an edge separating the window into two regions. Pixels i and j_1 have the same region index, but pixels i and j_2 have different region indexes [6]

- The unified energy function for kernel-based image denoising is proposed in [9] as:

$$E(\boldsymbol{z}) = (\boldsymbol{y} - \boldsymbol{z})^T F(K)(\boldsymbol{y} - \boldsymbol{z}) + \eta \boldsymbol{z}^T G(L) \boldsymbol{z} \qquad (7)$$

in which L is the corresponding Laplacian matrix computed from K, and η is a positive regularization parameter which balances the first term (data fidelity term) and the second term (smoothness term). Also, F(.) and G(.) are functions of K and L, to be specified shortly.

As we can see from [9], Substitution of F(K) = K and G(L) = L = D–K into equation (7) and minimizing the result with respect to z, results in the following closed form solution at convergence:

$$\boldsymbol{z} = [K + \eta L]^{-1} K \boldsymbol{y} \qquad (8)$$

where the (i, j)th element of matrix K is computed as:

$$K(i,j) = \exp\left(-\frac{\|\boldsymbol{y}_i - \boldsymbol{y}_j\|^2}{h^2}\right) \qquad (9)$$

where $\mathbf{y}_i$ is a vectorized noisy patch centered at pixel i and h is the smoothing parameter.

B. Proposed Algorithm

We start with some discussions on regularization parameter (η) which balances the data fidelity term and smoothness term in energy function exists in (7):

Remark I: Substitution of *F(K) = I* and *G(L) = L = D−K* into equation (7) minimizing the result with respect to *z*, results in the following closed form solution at convergence similar to equation (8),:

$$\boldsymbol{z} = [I + \eta(D - K)]^{-1}\boldsymbol{y} \tag{10}$$

comparison between (3) and (10) shows that the parameter η is set to be 2 in [18].

Since the structural features and contextual information differ from image to image, considering a constant value for η doesn't seem to be right.

Experimental results confirmed this fact as shown in **Error! Reference source not found.** and Fig. 4 which will be explained in section3.

Remark II: Since the structural features and information in the various areas of a single image are different, as indicated in Fig. 5, considering local values for the parameter η can improve the denoising performance.

Consequently, it is necessary to select the parameter η in equation (10) differently from pixel to pixel. Therefore, in this paper we introduce a diagonal matrix H to play this expanded role of η.

It is obvious that in [18] this diagonal matrix H is equivalent to 2I where I is the identity matrix.

In accordance with our discussion above, the proposed closed form solution in this paper is based on (8) as:

$$\boldsymbol{z} = [K + H(D - K)]^{-1}K\boldsymbol{y} \tag{11}$$

Remark III: In this work, we rewrite equation (10) as:

$$\boldsymbol{y} = \boldsymbol{z} + \eta(D - K)\boldsymbol{z} \tag{12}$$

comparison between Eq.(1) and Eq.(12) results in:

$$\boldsymbol{v} = \eta(D - K)\boldsymbol{z} \tag{13}$$

which shows the dependency of the parameter η to the noise (Fig. 6).

This will provide us with an insight into the determination of suitable value for η. We see that, as magnitude of noise increases, the suitable value of the parameter η typically gets larger. It is obvious from Eq. (2) and (7) that as magnitude of noise increases, the role of the second term (smoothness term) is more important to achieve the denoised image.

Through many choices of H, we determine this diagonal matrix as:

$$H_{ii} = var(\boldsymbol{y}_i) \tag{14}$$

where $\boldsymbol{y}_i$ is a vectorized noisy patch centered at pixel *i* and var(x) is the variance of the entries in the vector x.

The proposed algorithm is summarized as follows:

Input: an observed noisy image **y**

Output: a denoised image

Step 1: initialize algorithm parameters such as h, *c*

Step 2: compute the matrices K, D

Step 3: compute the matrix H from Eq. (14)

Step 4: construct the output image z from Eq. (11)

III. EXPERIMENTS AND EVALUATIONS

In this section, we start with three experiments on the parameter η. Then, to demonstrate the performance of our approach in the last experiment, we compare it with three algorithms: NLM [3], [18] and [18] which we have implemented them ourselves.

The eight gray level images (size: 216×216) used in the experiments are shown in Fig.2.

Fig. 2: The test images: Lena, Cameraman, Barbara, Peppers, Blood cell, Paint, Monarch and House.

Experiment I: In the first experiment, Gaussian white noise with a standard deviation 10 was added to each of the eight test images shown in Fig.2. Then, the closed form solutions based on Eq.(10) (with *K* from Eq. (4)) and also solution based on [9] were used individually to denoise each noisy test image.

PSNR of the denoised images were plotted for different values of the parameter η as shown in Fig. 3 and Fig. 4.

We can see that denoising algorithm based on Eq.(10) is more sensitive to the test image (and also to the parameter

η) than algorithm proposed in [9].

The optimal values of η corresponding to the highest PSNR for each test image are shown in Table I.

From this table, it is clear that in contrast to [18], the optimal global values of the parameter η are not generally the same for various images.

Experiment II: In the second experiment, Gaussian white noise with a standard deviation 10 was first added to Lena image. Then, the whole noisy image was partitioned into various patches (size: 32×32). Finally, the closed form solutions based on Eq.(10) and also [9] were used individually to denoise each noisy patch and the optimal η corresponding to the highest PSNR was achieved in each patch.

The plots of optimal values of η versus block (patch) numbers are shown in Fig. 5 for both methods.

From this figure, it is clear that the optimal values of the parameter η are different for various areas in a single image. We can see that the optimal value of η based on Eq.(10) is more sensitive to the local patch than algorithm proposed in [9].

According to this facts, locally determination of η is sensible.

Experiment III: In the third experiment, different levels of Gaussian white noise were first added to Lena image individually. Then, at each noise level, the closed form solutions based on Eq.(10) and also [9] were used individually to denoise this image.

The plots of optimal values of η versus standard deviation of noise are shown in Fig. 6 for both methods.

In Fig.7, PSNR of noisy and denoised images versus different levels of Gaussian white noise is illustrated. As we can see from this figure, in the high level of noise, the performance of the algorithm decreases.

Experiment IV: In the last experiment, we compare the proposed algorithm with three algorithms: NLM [3], [18] and [18] which we have implemented them ourselves.

In implementation of NLM [3], we set the search window size, the similarity window size and the filter degree to 15×15, 5×5 and 12 respectively. In [18], we set the parameters a and b to 5 and 114, repectively. In [9], the parameter η was fixed at 0.65 (the average of η values mentioned in [9]).

TABLE II exhibits the results on the noisy test images (σ_N = 10). Peak signal to noise ratio (PSNR) in dB and Structural Similarity (SSIM) are used as quantitative measures for comparison.

Fig. 8 illustrates House image denoised using the proposed approach compared to NLM [3], [18] and [18].

TABLE IIand Fig. 8 indicate that the results of our approach look much better than others

TABLE I: Optimal Global η Achieved by Using Eq.(10) and [9] Individually

Lena		Cameraman		Barbara		Peppers	
Eq. (10)	[9]	Eq. (10)	[9]	Eq. (10)	[9]	Eq. (10)	[9]
1.4	0.8	2.6	0.8	1.4	0.8	1.6	0.8
Bloodcell		Paint		Monarch		House	
Eq. (10)	[9]	Eq. (10)	[9]	Eq. (10)	[9]	Eq. (10)	[9]
1.6	1.0	1.6	0.8	1.6	1.0	2.4	1.0

TABLE II: Denoising PSNR Performance of the Proposed Algorithm

$(PSNR_N / \sigma_N) = (28.17 / 10)$	NLM [3]		[18]	
	PSNR	SSIM	PSNR	SSIM
Lena	32.69	0.91	31.20	0.87
Cameraman	33.33	0.92	32.61	0.90
Barbara	31.66	0.92	30.06	0.92
Peppers	32.89	0.89	31.61	0.86
Bloodcell	33.69	0.91	31.54	0.88
Paint	32.61	0.91	31.35	0.89
Monarch	32.80	0.94	31.53	0.91
House	34.42	0.88	32.77	0.85
Average	**33.01**	**0.91**	**31.58**	**0.88**

TABLE III: Denoising PSNR Performance of the Proposed Algorithm

$(PSNR_N / \sigma_N) = (28.17 / 10)$	[9]		Proposed	
	PSNR	SSIM	PSNR	SSIM
Lena	32.38	0.89	32.73	0.91
Cameraman	32.95	0.89	33.44	0.92
Barbara	31.37	0.91	31.72	0.92
Peppers	32.57	0.88	32.87	0.89
Bloodcell	33.15	0.90	33.82	0.91
Paint	32.26	0.90	32.66	0.92
Monarch	32.38	0.92	32.97	0.94
House	33.94	0.87	34.62	0.88
Average	**32.62**	**0.89**	**33.10**	**0.91**

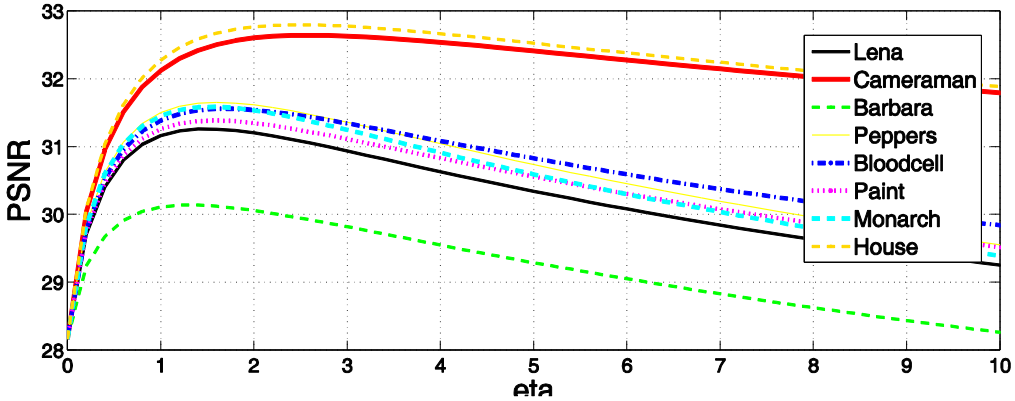

Fig. 3: PSNR results versus different values of the parameter η for the test images denoised based on Eq.(10).

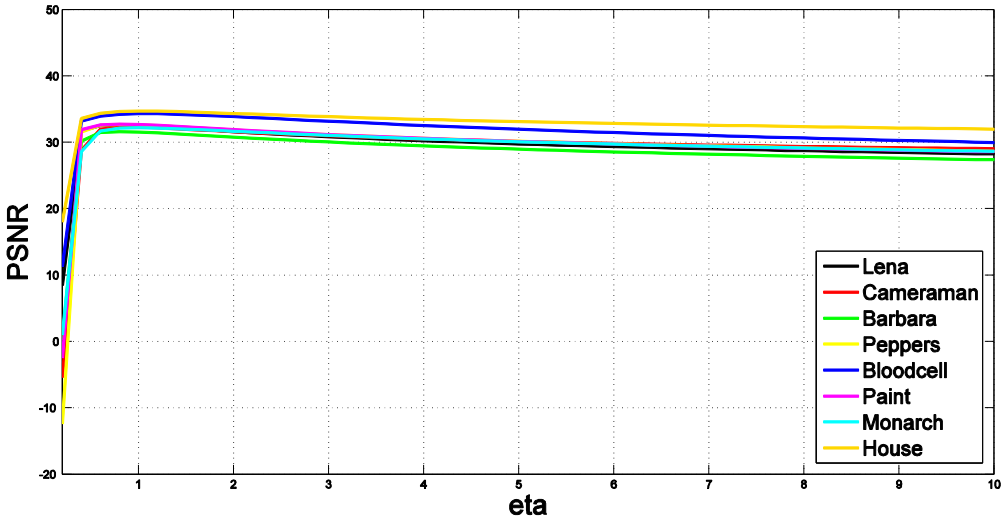

Fig. 4: PSNR results versus different values of the parameter η for the test images denoised based on [9].

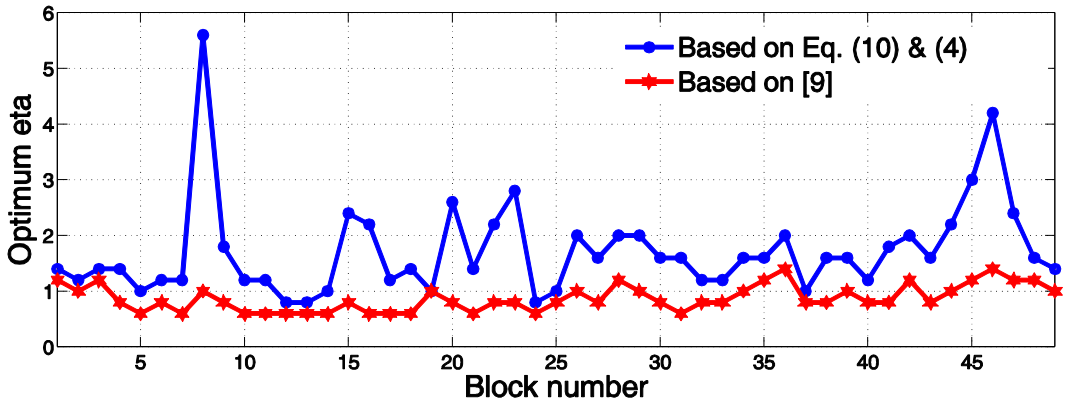

Fig. 5: Optimal values of η versus denoised block numbers using equation Eq.(10) and [9] individually.

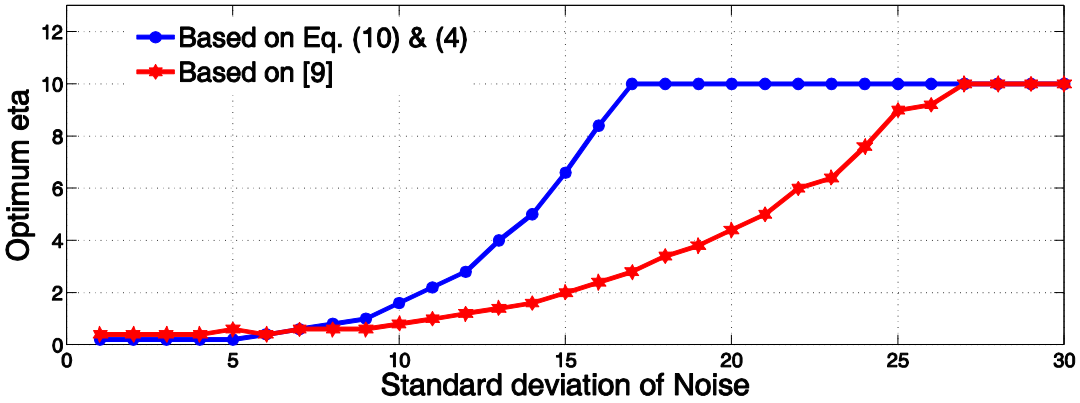

Fig. 6: Optimal values of η for denoised Lena image versus noise levels using Eq.(10) and [9] individually.

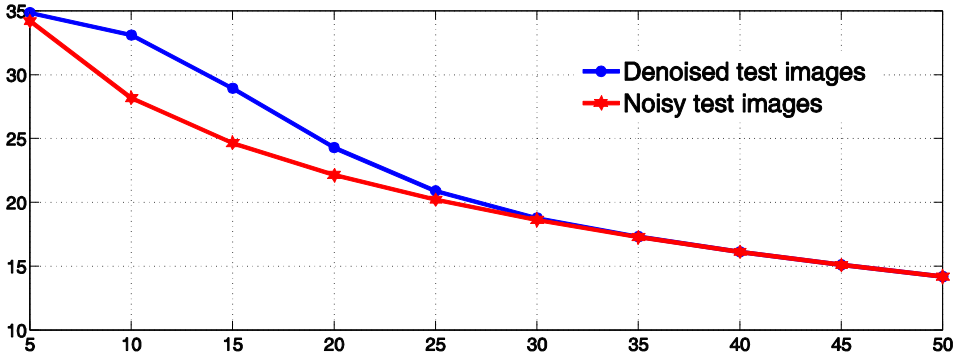

Fig. 7: PSNR of denoised image vs. Standard deviation of noise

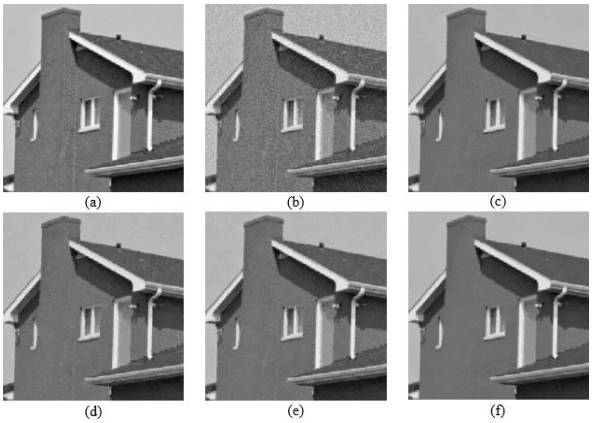

Fig. 8: Denoising experiment on 216×216 House image, (a) clean image, (b) noisy image (σ_N = 10), (c) standard NLM output image, (d) output image based on [18], (e) output image based on [9], (f) output image based on the proposed approach.

.

REFERENCES

[1] Ling Shao, Ruomei Yan, Xuelong Li and Yan Liu, "From Heuristic Optimization to Dictionary Learning: A Review and Comprehensive Comparison of Image Denoising Algorithms," IEEE transactions on cybernetics, vol. 44, no. 7, 2014.

[2] Ling Shao, Hui Zhang and Gerard de Haan, "An Overview and Performance Evaluation of Classification-Based Least Squares Trained Filters," IEEE transactions on image processing, vol. 17, no. 10, 2008.

[3] A. Buades and J. M. Morel Coll, "A nonlocal algorithm for image denoising," in Proc. IEEE Int. Conf. Comput. Vision Pattern Recognition, vol. 2. pp. 60–65, 2005.

[4] G. Peyre, "Image processing with nonlocal spectral bases," Multiscale Modeling & Simulation, vol. 7, no. 2, pp. 703–730, 2008.

[5] L. Pizarro, P. Mrazek, S. Didas, S. Grewenig, and J. Weickert, "Generalised nonlocal image smoothing," International Journal of Computer Vision, vol. 90, no. 1, pp. 62–87, 2010.

[6] P. Milanfar, "A tour of modern image filtering," IEEE Signal Process. Mag., vol. 30, no. 1, pp. 106–128, 2013

[7] A. Elmoataz, O. Lezoray, and S. Bougleux, "Nonlocal discrete regularization on weighted graphs: a framework for image and manifold processing," Image Processing, IEEE Transactions on, vol. 17, no. 7, pp. 1047–1060, 2008.

[8] D. Shuman, S. Narang, P. Frossard, A. Ortega, and P. Vandergheynst, "The emerging field of signal processing on graphs: Extending highdimensional data analysis to networks and other

irregular domains," Signal Processing Magazine, IEEE, vol. 30, no. 3, pp. 83–98, 2013

[9] Amin Kheradmand and Peyman Milanfar, "A General Framework for Kernel Similarity-based Image Denoising," IEEE Global Conference on Signal and Information Processing, 2013.

[10] Ning He, J. Wang, L. Zhang and K. Lu, "An improved fractional-order differentiation model for image denoising", signal Processing, vol. 12, pp. 180-188, 2015.

[11] J. Xu, A. Feng, Y. Hao, X. Zhang and Y. Han, "Image deblurring and denoising by an improved variational model", AEU - International Journal of Electronics and Communications, Vol. 70, Issue 9, pp. 1128–1133, 2016.

[12] E. P. Simoncelli, E. H. Adelson, A. Pizurica and W. Philips, "Noise removal via Bayesian wavelet coring," in Proc. IEEE Int. Conf. Image Process., pp. 379-382, 1996.

[13] M. Elad and M. Aharon, "Image denoising via sparse and redundant representations over learned dictionaries," IEEE Trans. Image Process.,vol. 15, no.12, pp. 3736–3745, 2006.

[14] M. Zhang, Ch. Desrosiers, "Image denoising based on sparse representation and gradient histogram", IET Image Processing, Vol. 11, Issue: 1, 2017.

[15] Q. Wang, X. Zhang, Y. Wu, L. Tang and Zh. Zha, "Non-Convex Weighted ℓp Minimization based Group Sparse Representation Framework for Image Denoising", IEEE Signal Processing Letters, Vol. , No. 99, 2017.

[16] Yibin Tang, Ying Chen, Ning Xu, Aimin Jiang, Lin Zhou, "Image denoising via sparse coding using eigenvectors of graph Laplacian, Digital Signal Processing", Vol. 50, pp. 114-122, 2016.

[17] Licheng Liu; Long Chen; C. L. Philip Chen; Yuan Yan Tang; Chi Man pun, "Weighted Joint Sparse Representation for Removing Mixed Noise in Image", IEEE Transactions on Cybernetics, Vol. 47, no. 3, 2017

[18] Shifeng Chen, Ming Liu, Wei Zhang and Jianzhuang Liu, "Edge preserving image denoising with a closed form solution," Pattern Recognition, Vol. 46, Issue 3, 2013.